Biometals (2008) 21:503–513
DOI 10.1007/s10534-008-9137-8

Investigation of ascorbate-mediated iron release from ferric phytosiderophores in the presence of nicotianamine

Günther Weber · Nicolaus von Wirén · Heiko Hayen

Received: 17 January 2008 / Accepted: 14 February 2008 / Published online: 6 March 2008

Abstract Phytosiderophores (PS) are strong iron chelators, produced by graminaceous plants under iron deficiency. The ability of released PS to chelate iron(III), and subsequent uptake of this chelate into roots by YS1-type transport proteins, are well-known. The mechanism of iron release from the stable chelate inside the plant cell, however, is unclear. One possibility involves the reduction of ferric PS in the presence of an iron(II) chelator via ternary complex formation. Here, the conversion of ferric PS species by ascorbate in the presence of the intracellular ligand nicotianamine (NA) has been investigated at cytosolic pH (pH 7.3), leading to the formation of a ferrous NA chelate. This reaction takes place when supplying Fe(III) as a chelate with 2′-deoxymugineic acid (DMA), mugineic acid (MA), and 3-*epi*-hydroxymugineic acid (*epi*-HMA), with the reaction rate decreasing in this order. The progress of the conversion of ferric DMA to ferrous NA was monitored in real-time by high resolution mass spectrometry (FTICR-MS), and the results are complemented by electrochemical measurements (cyclic voltammetry), which allows detecting reactive intermediates and their change with time at high sensitivity. Hence, the combined results of electrochemistry and mass spectrometry indicate an ascorbate-mediated mechanism for the iron release from ferric PS, which highlights the role of ascorbate as a simple, but effective plant reductant.

Keywords Phytosiderophores · Iron · Reduction · Cyclic voltammetry · Mass spectrometry

G. Weber (✉) · H. Hayen
ISAS-Institute for Analytical Sciences, Bunsen-Kirchhoff-Str. 11, 44139 Dortmund, Germany
e-mail: weber@isas.de

N. von Wirén
Institute of Plant Nutrition, Hohenheim University, Fruwirthstr. 20, 70599 Stuttgart, Germany

Introduction

Phytosiderophores (PS) of the mugineic acid (MA) family are small, aminocarboxylate-type iron chelators, which are produced by graminaceous plants in case of iron deficiency (Römheld and Marschner 1986; Treeby et al. 1989; Mori 1999). After excretion of PS from the roots, stable Fe(III)-chelates are formed, even in alkaline soils where the solubility of iron is extremely low. The undissociated ferric PS complex is then again taken up by YS1-type transport proteins, located in the root plasma membrane (Schaaf et al. 2004). This iron acquisition mechanism in grasses is called strategy II, and differs from strategy I, which is effective for all other plant species and relies mainly on increased proton secretion and Fe(III) reductase activity at the root plasma membrane for the subsequent uptake of Fe(II) by the IRT1 transporter (Schmidt 2003).

While the non-reductive uptake of ferric PS into grasses is well understood, the mechanism of further iron transport inside the plant remains unclear at present. Some potential ligands for iron (other than PS) have been postulated already, including small proteins (Krüger et al. 2002), citrate (Bienfait and Scheffers 1992; von Wirén et al. 1999), and nicotianamine (NA) (Ling et al. 1999; von Wirén et al. 1999; Hider et al. 2004), but the details of the respective processes are still unknown. Especially for NA, which is a direct precursor of PS in their biosynthetic pathway (Okumura et al. 1994; Kanazawa et al. 1994), there is some evidence for being involved in intracellular iron transport. However, a direct ligand exchange reaction of ferric PS with such ligands seems rather unlikely, because of the high thermodynamic stability of the ferric PS chelate. Hence, there must be another mechanism of iron release. One possible mechanism, which has been proposed already for bacterial siderophores (Halle and Meyer 1992; Andrews et al. 2003) and for ferric protein species (Griesen et al. 2004), involves the reduction of the ferric chelate by a physiological reducing agent, leading to the formation of the thermodynamically more labile ferrous chelate, which subsequently, or even simultaneously, may react with a suitable Fe(II) chelator (Boukhalfa and Crumbliss 2002; Mies et al. 2006). The practical relevance of such redox-mediated iron release or ligand exchange reactions has been demonstrated for iron bound to the bacterial siderophores ferrioxamine B (Mies et al. 2006) and pyoverdine (Greenwald et al. 2007), or to ferritins (Laulhere and Briat 1993; Sakurai et al. 2006) and bleomycin (Lovstad 1998). Hence, it seems reasonable to assume similar redox-mediated iron release reactions also for ferric PS. In fact, this has been suggested already more than twenty years ago as a consequence of the physico-chemical properties of the iron(III)-MA chelate (Sugiura et al. 1981), but experimental evidence has not yet been provided, to the best of our knowledge.

The main objective of the present study was to investigate the possibility of redox-mediated iron release from ferric PS under conditions simulating the plant cytoplasm and using ascorbate as physiological reducing agent and NA as ligand capable of stabilizing ferrous ions. Ascorbate is one of the primary antioxidants in plants (Noctor and Foyer 1998; Noctor 2006), and is available in the cytoplasm of plant cells at relatively high concentrations (up to the low millimolar level). Therefore, ascorbate has been used as reductant in several experiments on redox-mediated iron release (Lovstad 1998; Mies et al. 2006; Sakurai et al. 2006). NA was chosen as ligand, because there is strong evidence for an important role of this compound in the intracellular trafficking of iron (esp. in the ferrous state) and other metals, such as copper, nickel, zinc (Anderegg and Ripperger 1989; Stephan and Scholz 1993; von Wirén et al. 1999; Ouerdane et al. 2006). NA has also a similar chemical structure as PS, and forms iron chelates of comparable complex stability.

Accurate measurements of redox-mediated ligand exchange reactions require analytical methods, which enable a clear distinction between ferrous and ferric chelates of all ligands involved. Furthermore, the detection and unequivocal identification of previously unknown intermediates or byproducts should be possible at realistic (i.e. micromolar) concentrations. For kinetic measurements, obviously, the time scale of the measurement should be smaller than the progress of the reaction, which is monitored. Finally, the analytical method must not change the reactive species, which are formed during the reaction. This latter requirement excludes all methods which involve chromatographic (Ouerdane et al. 2006; Xuan et al. 2006) or electrophoretic (Xuan et al. 2007) separation of PS and related metal species, because such methods are only well-suited for relatively stable species, whereas labile or reactive intermediates would get lost during the separation process.

A method, which meets most of these requirements, and which has already been used successfully for the analysis of Fe(II)/Fe(III)-PS and -NA equilibria (Weber et al. 2006), is electrospray ionization—Fourier transform ion cyclotron resonance mass spectrometry (ESI-FTICR-MS). The use of FTICR-MS not only enables fast and direct measurements in complex reaction mixtures (without preceding separation), but it also provides the high resolution and mass accuracy, which is needed for unambiguous identification of all compounds detected, including ferrous and ferric chelates, free ligands, and reduced and oxidized forms of physiological reductants (e.g. ascorbate and dehydroascorbate).

Other methods, which have been used for monitoring the time course of redox and ligand exchange

reactions of iron chelates, include electron spin resonance (ESR) (Mouithys-Mickalad et al. 1998; van Duijn et al. 1998, 2000), fluorescence resonance energy transfer (FRET) (Greenwald et al. 2007), spectrophotometric (Xu and Jordan 1990; Lambert et al. 2004; Sakurai et al. 2006) and electrochemical measurements (Lambert et al. 2004; Boukhalfa and Crumbliss 2002). While ESR is very helpful for detecting radicals, a complete identification of unknown compounds is impossible with this method. The disadvantage of fluorescence or absorbance measurements lies in the fact, that they usually require the addition of special reagents, which may alter the chemical equilibria. Electrochemical techniques, namely cyclic voltammetry (CV), have been used frequently for the characterization of iron-siderophore chelates (Boukhalfa and Crumbliss 2002; Spasojevic et al. 1999), including PS and NA chelates (Sugiura et al. 1981; Mino et al. 1983). Since measured redox potentials directly reflect the redox state of iron and also the binding to chelating ligand(s), electrochemical methods are ideally suited for monitoring redox-mediated ligand exchange reactions. CV measurements do not provide complete structural information, but they may offer very high sensitivity for electrochemically reactive species even at low concentrations, which is an advantage over MS, especially in the case of very reactive intermediate products.

In the present study we have combined the two complementary methods MS and CV for the investigation of ascorbate-mediated iron release from ferric PS, resulting in the formation of ferrous NA. This reaction proceeds nearly instantaneously at physiological ascorbate concentrations, but is negligible in the absence of ascorbate. Moreover, the reaction rate is highly dependent on the hydroxylation state of PS, i.e. hydroxylated MA reacts much slower compared to deoxymugineic acid.

Materials and methods

All chemicals were of p.a. purity, unless stated otherwise. Solutions were prepared by using ultrapure water, which was obtained by passing through a Millipore Synergy 185 water purification system.

Phytosiderophores, nicotianamine, and respective iron chelates

The three PS 2′-deoxymugineic acid (DMA), MA, and 3-*epi*-hydroxymugineic acid (*epi*-HMA) were isolated and purified from plant cultures at the Institute of Plant Nutrition (Hohenheim University, Stuttgart, Germany). The respective concentrations in the purified standard solutions were determined by HPLC (Neumann et al. 1999). Nicotianamine was a kind gift from Profs. T. Kitahara and S. Mori (University of Tokyo, Japan). The purity of this chemically synthesized product was at least 95%, as confirmed by NMR.

Ferric PS chelates were prepared by addition of appropriate amounts of a freshly prepared iron stock solution to the respective PS dissolved in 50 mM acetate or carbonate buffer. If necessary, the pH was then readjusted to the desired value of 7.3.

Mass spectrometry

All MS experiments were carried out using a LTQ FT Fourier transform ion cyclotron resonance hybrid mass spectrometer (Thermo Fisher Scientific, Germany), equipped with a 7.0 T actively shielded superconducting magnet. The instrument was operated in negative ionization mode. Ion transmission into the linear trap and signal intensity was automatically optimized for maximum ion signal of the Fe(III)-DMA-chelate. The resolving power of the FTICR mass analyzer was set to 200,000 (FWHM at $m/z = 400$). Full scan FTICR mass spectra in the mass range $m/z = 100$–1000 were acquired using a single microscan. The instrument was calibrated externally using 0.01% solution of 85% phosphoric acid in water/methanol (1/1; v/v).

MS measurements were performed either by nano-electrospray using gold-plated emitters (2 μm inner tip diameter) filled with 5 μl of the sample, or by pneumatically assisted electrospray-ionization. For the latter, a syringe pump equipped with a 500 μl syringe was used at a flow rate of 6 μl/min enabling a monitoring time of more than 1 h for kinetic measurements.

To improve the comparability of different measurements, L-tryptophan (Roth, Germany) was added as an internal standard yielding a final concentration of 30 μM. All signal intensities were analyzed relative to the L-tryptophan signal intensity

(m/z = 203.0826). Before measurement, the samples were diluted with methanol (LC-MS grade, Riedel-de Haën, Germany) to 70% to avoid problems induced by high surface tension of pure water and to facilitate a stable spray at reduced needle voltage. The theoretical masses and isotope distributions for the iron chelates were calculated using the Xcalibur software LTQ FT version 1.4.2 (Thermo Fisher Scientific, USA).

Cyclic voltammetry

Electrochemical measurements were carried out using an Autolab PGSTAT20 (ECO Chemie, Netherlands), equipped with a Metrohm 663 VA-Stand (10 mL cell volume) with a 3 mm diameter boron-doped diamond rotating disk electrode (BDD-RDE, obtained from Windsor Scientific, UK) as working electrode, a Ag/AgCl/KCl (3 M) reference electrode, and a Pt counter electrode.

For the measurements of PS and Fe-PS samples, which are only available in very small amounts, a 'micro-volume-cell' was constructed, which is depicted in Fig. 1.

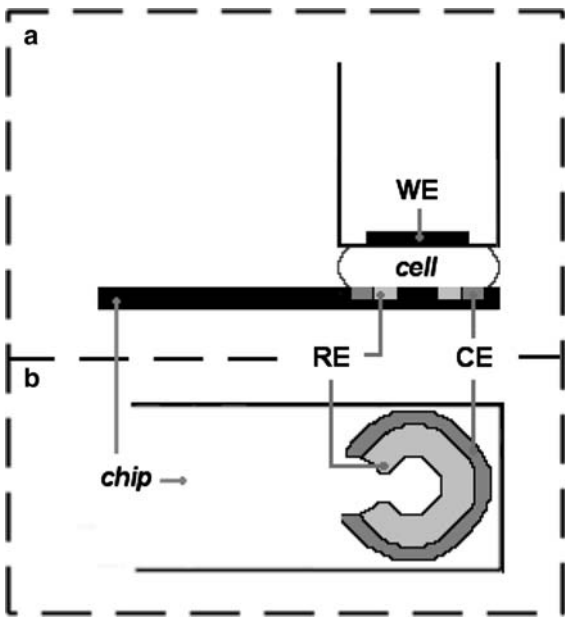

Fig. 1 Schematic diagram of the micro-volume electrochemical cell. (**a**) side view, (**b**) top view of electrode chip. WE: working electrode, RE: reference electrode, CE: counter electrode

The cell volume is formed by the space in between the BDD working electrode and a disposable electrode chip (obtained from BVT technologies, Czech Republic), which contains the Ag/AgCl reference and Au counter electrodes, as shown in Fig. 1. The cell is operated by removing the BDDE, putting a drop of 30 µl aqueous sample on to the electrode chip (such that all electrodes are in contact with the liquid), and finally re-positioning the BDDE at a fixed distance ($\sim$1 mm) above the chip, such that the BDDE is also in contact with the liquid sample. The whole electrochemical cell is housed in a Faraday cage and connected to the Autolab instrument for cyclic voltammetric measurements.

Results and discussion

In order to check for the possibility and relevance of ascorbate-mediated iron release reactions from ferric PS in the presence of the ligand NA, we performed a series of similar experiments with the three PS DMA, MA, and *epi*-HMA, using high-resolution mass spectrometry (nano-ESI-FTICR-MS) as the method of choice for detecting simultaneously all relevant chemical compounds in the mass-to-charge range of m/z = 100–1000. This method has been used already successfully for analysis of the quaternary system Fe(II)/Fe(III) plus DMA plus NA (Weber et al. 2006), but in this case the two ligands were mixed simultaneously with iron in both oxidation states, in the absence of ascorbate. Preferential formation of ferric DMA and ferrous NA was observed in these experiments, confirming the important role of NA as a candidate ligand for Fe(II).

Comparative experiments with three ferric PS chelates

In contrast to the previous experiments, we now started with a known amount (usually 10–30 µM) of one single ferric PS species at pH 7.3. After checking that a stable signal was measurable and no artefacts were produced during the measurement (in particular, no reduction of ferric compounds by the negative electrospray conditions), we added an equimolar amount of NA to the solution and, after waiting for 2 h, measured again, but no direct ligand exchange was observed for all three PS. Even after addition of a

ten-fold molar excess of NA, no detectable amounts of ferric or ferrous NA species were formed from ferric MA or ferric *epi*-HMA. Only for ferric DMA, which is the chelate with the lowest thermodynamic stability (von Wirén et al. 2000), a detectable but very small quantity of Fe(II)-NA was observed, which does not change considerably within several hours. Hence, a direct ligand exchange of ferric PS with NA is very unlikely to play a significant role in plants, at least at pH 7.3.

In contrast, addition of ascorbate at a concentration of 1–2 mM to a mixture of ferric PS and NA completely changed the situation (see Fig. 2).

Already after 1 min, which was the minimum time needed to place the sample solution in the nano-ESI capillary and to generate a stable spray, all three ferric PS have produced considerable amounts of the reaction product Fe(II)-NA. Apparently, ferric DMA reacts more rapidly (i.e. generates more Fe(II)-NA) than ferric MA, which, in turn, reacts more rapidly than ferric *epi*-HMA. This order of reaction rates was confirmed by repeated measurements of the same sample solutions 20 min later (see Fig. 2). In the case of ferric DMA, the respective values of Fe(II)-NA are nearly identical for 1 and 21 min, indicating that an equilibrium had been reached already after 1 min. For ferric MA, the Fe(II)-NA signal increased considerably within 20 min, but still did not reach the same level as observed for ferric DMA. A similar time-dependent evolution of Fe(II)-NA was seen for ferric *epi*-HMA, but at an even lower concentration level. As expected, dehydroascorbate (DHA, $m/z = 173.0092$), which is the main oxidation product of ascorbate, shows a similar trend as the major reaction product Fe(II)-NA. Its concentration increased with time in the case of ferric MA or *epi*-HMA supply, while it remained constant in the ferric DMA experiment. Although it must be noted that the ESI-MS measurements yield only semi-quantitative results, the simultaneous detection of two reaction products confirmed the possibility of an ascorbate-mediated iron release in the presence of an Fe(II) ligand. Even though a strong dependence of the reaction kinetics on the ferric PS ligand may be expected, the magnitude of this effect was surprisingly large. This may be explained, in principle, by the thermodynamic stabilities of the respective ferric species (von Wirén et al. 2000) which are inversely related to the ascorbate-mediated reaction rate.

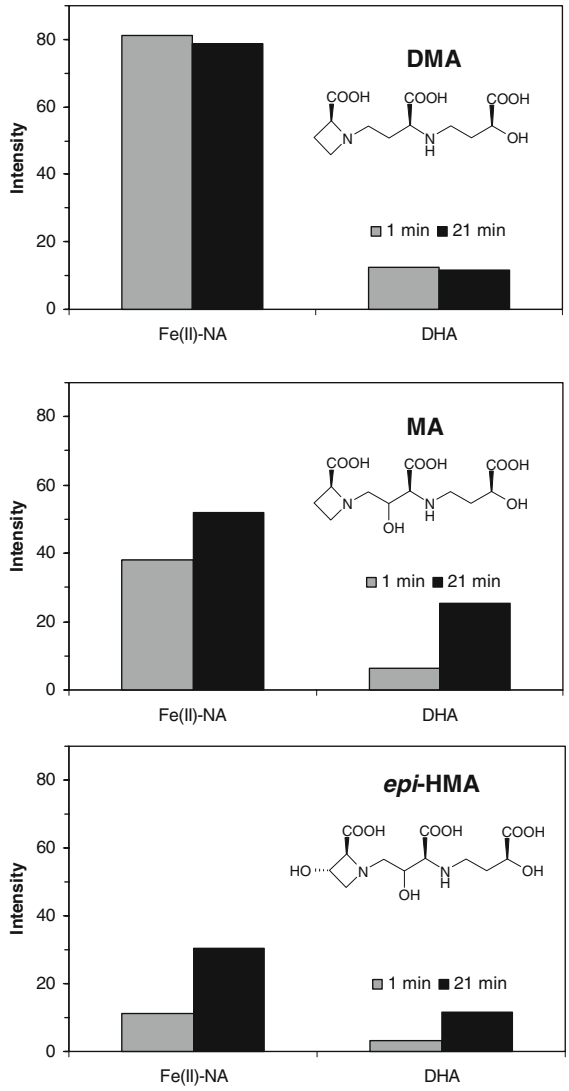

Fig. 2 Ascorbate-mediated formation of Fe(II)-NA from Fe(III)-DMA, Fe(III)-MA, and Fe(III)-*epi*-HMA, respectively, 1 and 21 min after ascorbate addition. DHA: formation of dehydroascorbate after reaction times of 1 and 21 min. Experiments were repeated several times with similar results, and representative results of one experiment are shown

Real-time monitoring of the ascorbate-mediated reaction of ferric DMA with NA

After having shown the possibility of ascorbate-mediated iron release from ferric PS under simulated physiological conditions, we wanted to investigate the mechanism of this reaction in more detail. For this purpose, we chose ferric DMA as example, because it reacts more readily than the other two ferric PS and

because more purified DMA was available for the experiments. After some initial experiments with the nano-ESI system we decided to use a syringe pump and a pneumatically assisted ESI interface for the kinetic measurements, since this enabled us to use up to 500 µl of sample solution at a flow rate of 6 µl/min, which is equivalent to a continuous monitoring time of more than one hour. The results of a typical kinetic measurement after addition of 600 µM ascorbate is depicted in Fig. 3.

It was clearly seen, that the increase of the Fe(II)-NA signal (at $m/z = 356.0551$) with time was accompanied by a respective decrease of the Fe(III)-DMA signal (at $m/z = 356.0312$). This result was expected, since the only iron source for Fe(II)-NA was Fe(III)-DMA, and one molecule of the product was formed from one molecule of the starting chelate, according to the (simplified) overall reaction:

$$\text{Fe(III)-DMA} + \text{NA} + \text{Asc} \leftrightarrow \text{Fe(II)-NA} + \text{DMA} + \text{MDHA},$$

or (since ascorbate is oxidized in two separate $1e^-/1H^+$ steps to DHA

$$2\text{Fe(III)-DMA} + 2\text{NA} + \text{Asc} \leftrightarrow 2\text{Fe(II)-NA} + 2\text{DMA} + \text{DHA}$$

with Asc = ascorbate, MDHA = monodehydroascorbate, and DHA = dehydroascorbate.

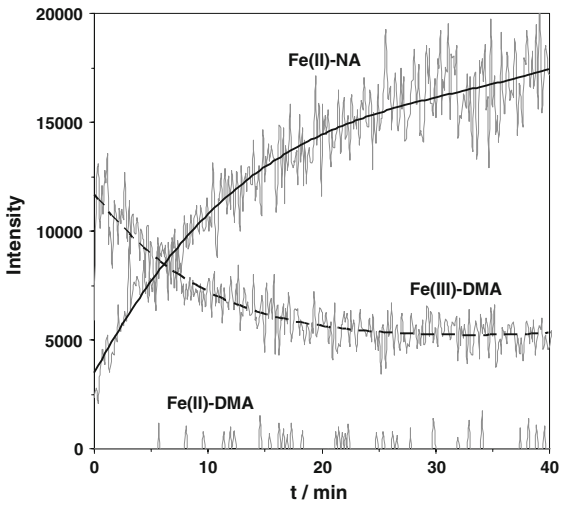

Fig. 3 Real-time monitoring of the ascorbate-mediated formation of Fe(II)-NA ($m/z = 356.0551$) and simultaneous decrease of Fe(III)-DMA ($m/z = 356.0312$) at pH 7.3 using ESI-FTICR-MS. Initial concentrations of Fe(III)-DMA, NA, and ascorbate were 30 µM, 30 µM, and 600 µM, respectively

According to the above equations, and also in full accordance with our results (but not shown in the figure), the progress of the reaction could also be monitored by following the increase of the free ligand DMA (at $m/z = 303.1198$), which was released from the ferric DMA chelate, or by the decrease of the free ligand NA (at $m/z = 302.1358$), which was consumed by formation of Fe(II)-NA. It is a clear advantage of the high resolution MS measurements, that all these species and several others (incl. Asc, MDHA, DHA) can be detected simultaneously, and—even more important—directly without any prior separation step. Another advantage of the analytical method is the unequivocal identification of the species, due to the high mass accuracy of the instrument. The identity of iron species was additionally confirmed by the characteristic isotopic pattern of iron.

There are, however, also limitations of the MS measurements. For example, it is usually assumed, that the first step in redox-mediated ligand exchange reactions is the reduction of the stable ferric species to the more labile ferrous species. However, as can be seen from Fig. 3, only traces of Fe(II)-DMA are detected at some time intervals, and in the first 6 min absolutely no Fe(II)-DMA could be detected. Unfortunately, it cannot be concluded from this result that Fe(II)-DMA is not an intermediate during the ligand exchange of iron. It could well be, that this species is present at a too low concentration and/or for too short time intervals to be detectable. Another possibility would be the formation of some kind of intermediate complex, which facilitates the redox reaction (Mies et al. 2006). Two reasonable intermediate species, which were in fact observed by MS are the ternary complexes [NA-Fe(III)-DMA] ($m/z = 659.1750$) and [Asc-Fe(III)-DMA] ($m/z = 532.0640$), but additional information is needed to verify a significant role of these adducts in the reaction pathway. It should be remembered, that the latter of the above iron species is undistinguishable (by MS) from the species [MDHA-Fe(II)-DMA], since the only difference of both structures is the electron distribution within the molecule.

Influence of the NA and ascorbate concentrations on reaction kinetics

In Table 1, the results of three experiments are shown, which only differ in the initial ascorbate concentration (300 or 600 µM), and in the initial NA

Table 1 Comparison of relative reaction rates and conversion efficiencies of ascorbate-mediated ligand exchange from Fe(III)-DMA to Fe(II)-NA

	Initial conc. (μM) Fe(III)-DMA:NA:Asc	Rel. reaction rate d/dt (Fe(II)-NA)	Conversion of Fe(III)-DMA after 25 min (%)
Exp.1	30:30:300	1.0	21
Exp.2[a]	30:30:600	2.5	48
Exp.3	30:150:600	3.7	56

[a] This is the experiment shown in Fig. 3

concentration (30 or 150 μM). Initial reaction rates were estimated from a linear approximation of the first 5 min of each reaction, and then normalized to that of the slowest reaction (Exp. 1), and the conversion efficiency of each reaction was estimated from the relative decrease of the initial Fe(III)-DMA concentration after 25 min.

Taking into account the noisy MS signals (see Fig. 3), it is clear that the values given in Table 1 should be taken only as rough estimates. They demonstrate, however, that a doubling of the ascorbate concentration from 300 to 600 μM has a much more pronounced effect on the reaction rate (factor 2.5) than a fivefold increase in NA concentration (the reaction rate of Exp. 3 differs only by a factor of 1.5 from that of Exp. 2). It is not surprising that the ascorbate concentration plays a key role in ascorbate-mediated reactions, but it must be remembered that ascorbate was already present in a ten-fold molar excess in Exp. 1. It thus seems that ascorbate is directly involved in the (rate-limiting) formation of an intermediate product/adduct.

Electrochemical experiments

Electroanalytical methods, in particular CV, have been used frequently to obtain information on redox-active species, including stable iron chelates (Shimizu et al. 2007), ferric siderophores (Spasojevic et al. 1999), and heme-proteins (Cowley et al. 2006). Also the mechanistic investigation of redox reactions involving ascorbate or other physiological reductants is possible (Graziano et al. 2002; Richter and Fischer 2006).

Hence, we applied CV as a complementary technique for the investigation of ascorbate-mediated ligand exchange reactions, because all major species involved (Fe(II)/(III)-PS, Fe(II)/(III)-NA, Asc/DHA) are electroactive. This is illustrated in Fig. 4a for the Fe(II)/(III)-NA-couple, and in Fig. 4b for the irreversible oxidation of ascorbate. Both CVs were measured at pH 7.3 using a BDDE as working electrode versus Ag/AgCl as reference. A BDDE was chosen as working electrode because of its very low and stable background currents, low susceptibility for electrode-fouling reactions, and high overpotentials for oxygen and hydrogen evolution.

Fe(II)/(III)-NA exhibits a well-defined quasi-reversible one-electron redox process, with a midpoint potential of +0.065 V and a peak current ratio (Ip,a/Ip,c) of 1.05. For comparison, also the ferri-/ferrocyanide couple was measured (not shown), and a midpoint potential of +0.206 V was obtained, which is in good agreement with the expected value (Kuta and Yeager 1975). The completely irreversible oxidation of ascorbate (see Fig. 4b), as well as its high

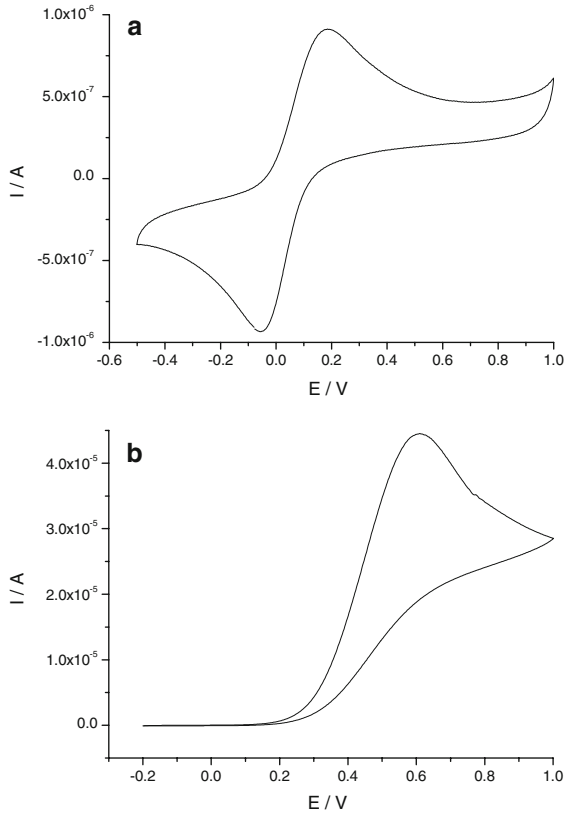

Fig. 4 Cyclic voltammograms of (**a**) 100 μM Fe(II)/(III)-NA, and (**b**) 1 mM ascorbate at a BDDE in 0.1 M sodium acetate, adjusted to pH 7.3. The standard electrochemical cell was used. Scan rate: 100 mV/s

overpotential, are well known for several electrode materials (Safavi et al. 2006; Nassef et al. 2007). The peak potential of +0.610 V vs. Ag/AgCl is in good agreement with that reported recently for ascorbate at a BDDE (Radovan et al. 2006).

For kinetic measurements, which are comparable to the kinetic MS measurements, we used the micro-volume-cell (see "Material and methods"), with 30 µl of sample solution at a slightly higher initial concentration of Fe(III)-DMA (100 µM). Similar to the MS measurements, we did not measure significant ligand exchange of Fe(III)-DMA after addition of an equimolar concentration of NA, but after addition of 500 µM ascorbate, the CV changed completely, as shown in Fig. 5a.

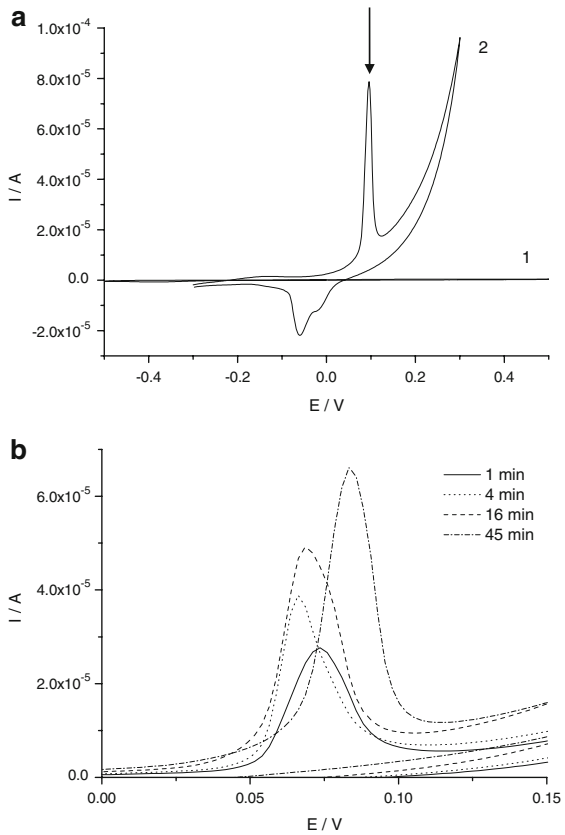

Fig. 5 (**a**) Cyclic voltammograms of a mixture of 100 µM Fe(III)-DMA and 100 µM NA (1) before, and (2) after addition of 500 µM ascorbate. The electrochemical micro-volume-cell was used. Scan rate: 100 mV/s. The arrow marks the new anodic peak, which was used for monitoring the on-going reaction (**b**) details of the cyclic voltammograms recorded after 1, 4, 16, and 45 min after ascorbate addition to the system Fe(III)-DMA plus NA. The anodic peak corresponds to that in Fig. 5a, marked by an arrow

A new anodic peak appeared (marked by an arrow), which is boosted to the 80 µA range (compared to less than 1 µA for the largest peak in the mixture of Fe(III)-DMA plus NA; the CV of this mixture is recognized in Fig. 5a only as a horizontal 'zero' line). Note, that only the onset of ascorbate oxidation is visible in Fig. 5a, because the scan was reversed already at +0.3 V, but it was checked, that the peak maximum for ascorbate oxidation is still at +0.61 V. Hence, the new peak is not attributable to the oxidation of free ascorbate, although it is somehow related to ascorbate oxidation—but only in the presence of the Fe(III)-DMA/NA mixture. A reasonable explanation for this behaviour is given by the 'catalytic' oxidation of that part of ascorbate, which is chemically linked (e.g. as an adduct) to the on-going reaction of ferric PS to ferrous NA. There are several examples in the literature for 'catalytic' systems, that are able to significantly reduce the high overpotential of ascorbate oxidation (Nalini and Narayanan 2000; Raoof et al. 2001; Chen et al. 2007; Wang et al. 2007). Interestingly, these catalytic systems employ metal-chelates as catalysts.

The hypothesis that the new peak is due to an electrocatalytic adduct, which is directly involved in the ascorbate-mediated ligand exchange reaction, is supported by the observation, that the peak changes with time (Fig. 5b). While the anodic peak current increases continuously with time, the peak potential shifted negatively for reaction times up to 5 minutes, and then shifted back for longer reaction times. In Fig. 6a and b these findings were compared to the above mentioned results from the high resolution MS.

In Fig. 6a, the increase of the anodic peak current Ip with time is compared to the respective increase of the MS signal of Fe(II)-NA, which is indicative of the progress of the (overall) reaction. Although only few data points are present for the Ip measurement (due to the fact, that we wanted to record full CVs and not only the peak current), a good correlation between both measurements was obtained. In contrast to this steady and simultaneous increase of Fe(II)-NA formation and peak current, Fig. 6b shows a very sharp decrease of the electrochemical peak potential in the first 2–4 min, followed by a slow back-shift to more positive potentials. This time course was compared with that of the species [DMA-Fe(III)-Asc] = [DMA-Fe(II)-MDHA], as measured by MS. Although the MS measurement was very noisy (due to the low

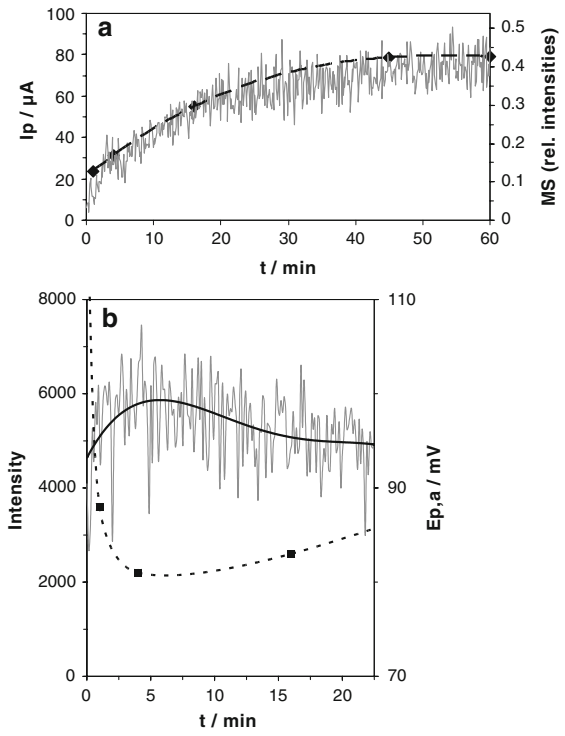

Fig. 6 (**a**) Change of anodic peak current Ip of the new peak (see Fig. 5) with time (dashed line), and corresponding MS monitoring of Fe(II)-NA (**b**) change of anodic peak potential Ep,a of the new peak (see Fig. 5) with time (dashed line), and corresponding MS monitoring of the adduct of Fe(III)-DMA with ascorbate ($m/z = 532.0633$, solid line)

concentration of this intermediate), the similarity of both measurements became evident at a maximum/minimum at about 4 min. This supports the hypothesis, that the formation of an ascorbate adduct of ferric PS and an intramolecular iron reduction are the first, rate-limiting steps in the ascorbate-mediated reaction, which then proceeds by a direct reaction of the ferrous adduct with NA to form the stable end product. At present, it cannot be fully excluded that the reaction may be initiated alternatively by the formation of the ternary complex DMA-Fe(III)-NA, which then reacts in a rate-limiting step with ascorbate (according to the mechanism proposed for iron release from ferrioxamine B in the presence of the Fe(II) chelator bathophenanthroline (Mies et al. 2006)). In this case, however, the ascorbate adduct should already contain NA, and also a strong correlation with the initial NA concentration would be expected, which was not the case in our experiments (see Table 1).

Concluding remarks

The combination of electrochemical and mass spectrometric methods facilitated a more detailed investigation of the ascorbate-mediated ligand exchange reaction. As a result, a reasonable mechanism for the iron release from ferric PS is proposed, which highlights the role of ascorbate as an efficient reductant in plants.

Acknowledgements We thank E. Scheuermann (Hohenheim University, Germany) for supply of purified phytosiderophores, Profs. T. Kitahara and S. Mori (University of Tokyo, Japan) for supply of synthesized NA, and the *Deutsche Forschungsgemeinschaft* for financial support to GW (grants WE 2422/5) and to NvW (grants WI 1728/6). Financial support from the *Ministerium für Innovation, Wissenschaft, Forschung und Technologie des Landes Nordrhein-Westfalen* and by the *Bundesministerium für Bildung und Forschung* is gratefully acknowledged.

References

Anderegg G, Ripperger H (1989) Correlation between metal complex formation and biological activity of nicotianamine analogues. J Chem Soc Chem Commun 647–650

Andrews SC, Robinson AK, Rodriguez-Quinones F (2003) Bacterial iron homeostasis. FEMS Microbial Rev 27:215–237

Bienfait HF, Scheffers MR (1992) Some properties of ferric citrate relevant to the iron nutrition of plants. Plant Soil 143:141–144

Boukhalfa H, Crumbliss AL (2002) Chemical aspects of siderophore mediated iron transport. Biometals 15:325–339

Chen SM, Chen JY, Thangamuthu R (2007) Electrochemical preparation of poly(malachite green) film modified Nafion-coated glassy carbon electrode and its electrocatalytic behavior towards NADH, dopamine and ascorbic acid. Electroanalysis 19:1531–1538

Cowley AB, Kennedy ML, Silchenko S, Lukat-Rodgers GS, Rodgers KR, Benson DR (2006) Insight into heme protein redox potential control and functional aspects of six-coordinate ligand-sensing heme proteins from studies of synthetic heme peptides. Inorg Chem 45:9985–10001

Graziano M, Biligni MV, Lamattina L (2002) Nitric oxide improves internal iron availability in plants. Plant Physiol 130:1852–1859

Greenwald J, Hoegy F, Nader M, Journet L, Mislin GLA, Graumann PL, Schalk IJ (2007) Real time fluorescent resonance energy transfer visualization of ferric pyoverdine uptake in *Pseudomonas aeruginosa*. J Biol Chem 282:2987–2995

Griesen D, Su D, Bérczi A, Asard H (2004) Localization of an ascorbate-reducible cytochrome b561 in the plant tonoplast. Plant Physiol 134:726–734

Halle F, Meyer JM (1992) Iron release from ferrisiderophores. A multi-step mechanism involving a NADH/FMN oxidoreductase and a chemical reduction by $FMNH_2$. Eur J Biochem 209:621–627

Hider RC, Yoshimura E, Khodr H, von Wirén N (2004) Competition or complementation: the iron-chelating abilities of nicotianamine and phytosiderophores. New Phytol 164:204–208

Kanazawa K, Higuchi K, Nishizawa NK, Fushiya S, Chino M (1994) Nicotianamine aminotransferase activities are correlated to the phytosiderophore secretions under Fe-deficient conditions in Gramineae. J Exp Bot 45:1903–1906

Krüger C, Berkowitz O, Stephan UW, Hell R (2002) A metal-binding member of the late embryogenesis abundant protein family transports iron in the phloem of *Ricinus communis L.* J Biol Chem 277:25062–25069

Kuta J, Yeager E (1975) The influence of cations on the electrode kinetics of ferricyanide-ferrocyanide system on the rotating gold electrode. J Electroanal Chem 59:110–112

Lambert F, Policar C, Durot S, Cesario M, Yuwei L, Korri-Youssoufi H, Keita B, Nadjo L (2004) Imidazole and imidazolate iron complexes: on the way for tuning 3D-structural characteristics and reactivity. Redox interconversions controlled by protonation state. Inorg Chem 43:4178–4188

Laulhere JP, Briat JF (1993) Iron release and uptake by plant ferritin: effects of pH, reduction and chelation. Biochem J 290:683–699

Ling HQ, Koch G, Bäumlein H, Ganal MW (1999) Map-based cloning of chloronerva, a gene involved in iron uptake of higher plants encoding nicotianamine synthase. Proc Natl Acad Sci USA 96:7098–7103

Lovstad RA (1998) Stimulatory effect of ascorbate on iron transfer from bleomycin to apotransferrin. Biometals 11:199–202

Mies KA, Wirgau JI, Crumbliss AL (2006) Ternary complex formation facilitates a redox mechanism for iron release from a siderophore. Biometals 19:115–126

Mino Y, Ishida T, Ota N, Inoue M, Nomoto K, Takemoto T, Tanaka H, Sugiura Y (1983) Mugineic acid-Iron(III) complex and its structurally analogous cobalt(III) complex: characterization and implications for absorption and transport of iron in gramineous plants. J Am Chem Soc 105:4671–4676

Mori S (1999) Iron acquisition by plants. Curr Opin Plant Biol 2:250–253

Mouithys-Mickalad A, Deby C, Deby-Dupont G, Lamy M (1998) An electron spin resonance (ESR) study on the mechanism of ascorbyl radical production by metal-binding proteins. Biometals 11:81–88

Nalini B, Narayanan SS (2000) Amperometric determination of ascorbic acid based on electrocatalytic oxidation using a ruthenium(III) diphenyldithiocarbamate-modified carbon paste electrode. Anal Chim Acta 405:93–97

Nassef M, Radi AE, O'Sullivan C (2007) Simultaneous detection of ascorbate and uric acid using a selectively catalytic surface. Anal Chim Acta 583:182–189

Neumann G, Haake C, Römheld V (1999) Improved HPLC method for determination of phytosiderophores in root washings and tissue extracts. J. Plant Nutr 22:1389–1402

Noctor G (2006) Metabolic signalling in defence and stress: the central roles of soluble redox couples. Plant Cell Environ 29:409–425

Noctor G, Foyer CH (1998) Ascorbate and glutathione: keeping active oxygen under control. Annu Rev Plant Physiol Plant Mol Biol 49:249–279

Okumura N, Nishizawa NK, Umehara Y, Ohata T, Nakanishi H, Yamaguchi T, Chino M, Mori S (1994) A dioxygenase gene (*Ids2*) expressed under iron deficiency conditions in the roots of *Hordeum vulgare*. Plant Mol Biol 25:705–719

Ouerdane L, Mari S, Czernic P, Lebrun M, Lobinski R (2006) Speciation of non-covalent nickel species in plant tissue extracts by electrospray Q-TOFMS/MS after their isolation by 2D size exclusion-hydrophilic interaction LC (SEC-HILIC) monitored by ICP-MS. J Anal At Spectrom 21:676–683

Radovan C, Manea F, Ciorba A, Cinghita D, Vlaicu I, Murariu M (2006) Some practical aspects regarding an application of the amperometric oxidability level concept in characterisation of waste water. Proceedings of the 13th symposium on analytical and environmental problems, Szeged, pp 265–269

Raoof JB, Ojani R, Kiani A (2001) Carbon paste electrode spiked with ferrocene carboxylic acid and its application to the electrocatalytic determination of ascorbic acid. J Electroanal Chem 515:45–51

Richter Y, Fischer B (2006) Nucleotides and inorganic phosphates as potential antioxidants. J Biol Inorg Chem 11:1063–1074

Römheld V, Marschner H (1986) Evidence for a specific uptake system for iron phytosiderophores in roots of grasses. Plant Physiol 80:175–180

Safavi A, Maleki N, Moradlou O, Tajabadi F (2006) Simultaneous determination of dopamine, ascorbic acid, and uric acid using carbon ionic liquid electrode. Anal Biochem 359:224–229

Sakurai K, Nabeyama A, Fujimoto Y (2006) Ascorbate-mediated iron release from ferritin in the presence of alloxan. Biometals 19:323–333

Schaaf G, Ludewig U, Erenoglu BE, Mori S, Kitahara T, von Wirén N (2004) ZmYS1 functions as a proton-coupled symporter for phytosiderophore- and nicotianamine-chelated metals. J Biol Chem 279:9091–9096

Schmidt W (2003) Iron solutions: acquisition strategies and signaling pathways in plants. Trends Plant Sci 8:188–193

Shimizu K, Hutcheson R, Engelmann MD, Cheng IF (2007) Cyclic voltammetric and aqueous equilibria model study of the pH dependant iron(II/III)ethylenediamminetetraacetate complex reduction potential. J Electroanal Chem 603:44–50

Spasojevic I, Armstrong SK, Brickman TJ, Crumbliss AL (1999) Electrochemical behavior of the Fe(III) complexes of the cyclic hydroxamate siderophores alcaligin and desferrioxamine E. Inorg Chem 38:449–454

Stephan UW, Scholz G (1993) Nicotianamine: mediator of transport of iron and heavy metals in the phloem? Physiol Plant 88:522–529

Sugiura Y, Tanaka H, Mino Y, Ishida T, Ota N, Inoue M (1981) Structure, properties, and transport mechanism of iron(III) complex of mugineic acid, a possible phytosiderophore. J Am Chem Soc 103:6979–6982

Treeby M, Marschner H, Römheld V (1989) Mobilization of iron and other micronutrient cations from a calcareous soil by plant-borne, microbial, and synthetic metal chelators. Plant Soil 114:217–226

van Duijn MM, Tijssen K, van Steveninck J, van den Broek PJA, van der Zee J (2000) Erythrocytes reduce extracellular ascorbate free radicals using intracellular ascorbate as an electron donor. J Biol Chem 275:27720–27725

van Duijn MM, van der Zee J, vanSteveninck J, van den Broek PJA (1998) Ascorbate stimulates ferricyanide reduction in HL-60 cells through a mechanism distinct from the NADH-dependent plasma membrane reductase. J Biol Chem 273:13415–13420

von Wirén N, Klair S, Bansal S, Briat JF, Khodr H, Shioiri T, Leigh RA, Hider RC (1999) Nicotianamine chelates both FeIII and FeII. Implications for metal transport in plants. Plant Physiol 119:1107–1114

von Wirén N, Khodr H, Hider RC (2000) Hydroxylated phytosiderophore species possess an enhanced chelate stability and affinity for iron(III). Plant Physiol 124:1149–1157

Wang B, Noguchi T, Anzai JI (2007) Layer-by-layer thin film-coated electrodes for electrocatalytic determination of ascorbic acid. Talanta 72:415–418

Weber G, von Wirén N, Hayen H (2006) Analysis of iron(II)/iron(III) phytosiderophore complexes by nano-electrospray ionization Fourier transform ion cyclotron resonance mass spectrometry. Rapid Commun Mass Spectrom 20:973–980

Xu J, Jordan RB (1990) Knietics and mechanism of the reaction of aqueous iron(III) with ascorbic acid. Inorg Chem 29:4180–4184

Xuan Y, Scheuermann EB, Meda AR, Hayen H, von Wirén N, Weber G (2006). Separation and identification of phytosiderophores and their metal complexes in plants by zwitterionic hydrophilic interaction liquid chromatography coupled to electrospray ionization mass spectrometry. J Chromatogr A 1136:73–81

Xuan Y, Scheuermann EB, Meda AR, Jacob P, von Wirén N, Weber G (2007) CE of phytosiderophores and related metal species in plants. Electrophoresis 28:3507–3519